WATER RESEARCH 44 (2010) 3055–3064

Available at www.sciencedirect.com

ScienceDirect

journal homepage: www.elsevier.com/locate/watres

Residual aluminium in water defluoridated using activated alumina adsorption – Modeling and simulation studies

Suja George[a,*], *Prabhat Pandit*[a], *A.B. Gupta*[b]

[a] *Department of Chemical Engineering, Malaviya National Institute of Technology Jaipur, J. L. N. Marg, Jaipur, Rajasthan 302017, India*
[b] *Department of Civil Engineering, Malaviya National Institute of Technology Jaipur, J. L. N. Marg, Jaipur, Rajasthan 302017, India*

ARTICLE INFO

Article history:
Received 22 April 2009
Received in revised form
18 February 2010
Accepted 18 February 2010
Available online 26 February 2010

Keywords:
Defluoridation
Residual aluminium
Activated alumina
Adsorption
Fluoride
Dissolved aluminium

ABSTRACT

The removal of fluoride from drinking water by the method of adsorption on activated alumina is found superior than other defluoridation techniques mostly due to the strong affinity between aluminium and fluoride. Dissolution of aluminium from the alumina surfaces into its free and hydroxide ions in the aqueous medium is reported to be very low, but the presence of high fluoride concentrations may increase its solubility due to the formation of monomeric aluminium fluoride and aluminium hydroxyl fluoride complexes. An Activated Alumina Defluoridation Model Simulator (AAD) has been developed to represent fluoride adsorption on the basis of the surface complexation theory incorporating aspects of aluminium solubility in presence of high fluoride concentrations and pH variations. Model validations were carried out for residual aluminium concentrations in alumina treated water, by conducting a series of batch fluoride adsorption experiments using activated alumina (grade FB101) treating fluoride concentrations of 1–10 mg/L, at varying pH conditions. The total residual aluminium in the defluoridated water is due to presence of both dissolved and precipitated Al–F complexed forms. The Freundlich adsorption isotherm was found fit for fluoride adsorption capacity *versus* residual fluoride concentrations for pH = 7.5, and the relationship is given by the linearised equation $\log(x/m) = \log k + (1/n) \log C_e$ with values of $k = 0.15$ mg/g and $1/n = 0.45$ indicating favorable adsorption. The relationship is linear in the region of low fluoride concentrations, but as concentrations of fluoride increased, the formation of the dissolved AlF_3^0 complexes was favored than adsorption on alumina, and hence makes the isotherm nonlinear. The AAD simulations can predict for operating fluoride uptake capacity in order to keep the residual aluminium within permissible limits in the alumina treated water.

1. Introduction

Aluminium based adsorbents such as poly aluminium chloride, poly aluminium hydroxyl sulphate, alum sludge (aluminium hydroxides), activated alumina and alumina impregnated with various oxides (manganese, magnesium, ferric hydroxides etc) are found to be suitable for defluoridation of water because of factors such as high affinity between fluorine and aluminium, porosity, availability of large number of surface active sites etc when compared to other defluoridation methods. The solubility of aluminium from the alumina surface when it is used in water treatment around the neutral pH range, is reported to be very low, (as solubility product value (K_{SP}) of aluminium oxides is 10^{-32}) but presence of high fluorides in raw water and variation in pH may cause the dissolution of more aluminium into the treated water

---

[*] *Corresponding author.*
E-mail address: soojamnit@yahoo.co.in (S. George).

0043-1354/$ – see front matter © 2010 Elsevier Ltd. All rights reserved.
doi:10.1016/j.watres.2010.02.028

during the defluoridation process. Presence of high fluorides in groundwater is a major problem in India as well as in many areas of the world including Canada, large parts of Africa, China, Middle East and southern Asia. The natural level of groundwater fluoride has been reported to be as high as 95 mg/L in Tanzania waters, 23 mg/L in Karbi Anglong district of Assam, and 30 mg/L in Barmer district of Rajasthan in India. Aluminium was earlier regarded as a relatively innocuous element but recent research has found that its various bound forms with the fluoride and other inorganic/organic ions are toxic in nature. Aluminium is a potential neuro-toxic agent in human beings and studies of Martyn et al. (1989), McLachlan et al. (1991), Berend and Trouwborst (1999), Strunecka and Patocka (1999) and Gauthier et al. (2000) have demonstrated relationships between aluminium and aluminium fluorides in drinking water and Alzheimer's disease. The permissible dissolved aluminium concentrations in treated drinking water under the USEPA secondary drinking water regulation is 0.05–0.2 mg/L Al (USPHS, 1987) and WHO suggestion (1997) and Indian Regulation IS10500 (1991) is maximum of 0.2 mg/L.

Activated alumina based domestic defluoridation units and community level hand pump attached defluoridation units are presently the most widely accepted defluoridation method in Indian villages having groundwater fluoride concentrations greater than 5 mg/L. It is reported that for conditions around neutral pH, residual aluminium concentrations are present in alumina treated waters in the range of 0.1–0.3 mg/L (using alumina columns) by Agarwal et al. (1999) and 0.01–0.05 mg/L (in AA domestic defluoridation units) by Kumar and Verma (2004). A dissolution rate model had been developed for hydrated γ-alumina adsorbents by Lefevre et al. (2004) on the basis of experimental studies for alkaline and acid conditions and reported that the dissolved aluminium concentrations varied from 4.86 mg/L to 17.82 mg/L for time period of 2–22 h for the acidic ($pH < 3$) and alkaline ($pH > 9$) pH ranges. Sanjuan and Michard (1987) experimented on aluminium hydroxide solubility in aqueous solutions containing fluoride ions at 50 °C and reported that aluminium fluoride complexes are important in aluminium solubility in acidic conditions when fluoride concentrations exceeds 10^{-3} M. In view of the wide application of alumina based defluoridation methods and with findings of synergistic toxicity of aluminium and fluoride, this paper presents the Activated Alumina Defluoridation model simulator (AAD) developed on the basis of the surface complexation theory incorporating aspects of aluminium solubility and reports the detailed experimental batch studies conducted at Malaviya National Institute of Technology Jaipur for validations of residual aluminium concentrations in alumina treated water.

2. Development of theoretical model

The activated alumina surface is composed of a number of discrete sites that consist of mobile H^+ ions that can go from surface to solution, while the surface acquires charge in the aqueous medium. The 2 p*K* surface complexation models are used to represent their surface ionization behavior and complexation with the adsorbed species (Feltes and Timmons, 2005; Todorovic and Milonjovic, 2004). Fluoride adsorption occurs as a result of its preferential adsorption onto the oxide surfaces and formation of complexes between the fluoride ions and the positively charged sites. Hiemstra and VanRiemsdijk (2000) studied adsorption and transport of fluoride by variable charge surfaces on goethite and silica for variable pH and reported that formation of the fluoride surface complex is accompanied by a redistribution of charge, and the OH/F exchange can be considered as fully located on the surface. The adsorption capacity is reported to vary directly with increase in fluoride concentration and inversely with pH of the solution (Valdivieso et al., 2005; Singh et al., 2005). Effect of varying pH and high fluoride concentrations on the aluminium solubility from the alumina surfaces during the defluoridation process was studied and following set of model equations have been used to represent alumina defluoridation in the Activated Alumina Defluoridation model simulator (AAD). The hypotheses and the sequence of reactions leading to the development of this model simulator are as follows:

- The alumina surface offers a plane for Al–F complexation reactions leading to defluoridation of water, which in turn, depends on the surface site density and surface potential at the adsorption plane. The extent of surface ionization into its positively or negatively charged surface sites will depend on the pH of the aqueous medium.
- Aluminium will dissolve from the alumina surface undergoing equilibrium dissolution with respect to the pH and the residual fluoride concentrations in the treated water. The total aluminium transferred to the treated water will include the charged dissolved forms and the neutral precipitated forms that remain suspended due to their colloidal sizes in ranges less than 2 μm. The dissolved aluminium consists of Al–F complexes such as AlF^{2+}, AlF_2^+, AlF_4^-, AlF_5^{2-} and AlF_6^{3-}, aluminium hydroxyl fluorides like $AlOHF^+$, $Al(OH)_2F_2^-$, forms of free Al^{3+} and hydroxides like $AlOH^{2+}$, $Al(OH)_2^+$, $Al(OH)_4^-$ and $Al_2(OH)_2^{2+}$ etc. The neutral precipitates include complexes like AlF_3^0, $AlOHF_2^0$, $Al(OH)_2F^0$ and $Al(OH)_3^0$. The adsorbed fluoride is in the form of $[\equiv AlOH_2F^0]$.

The surface complexation theory represents the alumina surface behavior, site densities, potential at the adsorption plane and fluoride complexation reaction in the defluoridation mechanism. The charging mechanism of the aluminium oxide surface due to its amphoteric nature can be both by adsorption and desorption of protons and is represented by following equations:

$$\equiv AlOH + H^+ \overset{K_1}{\leftrightarrow} \equiv AlOH_2^+ \tag{1}$$

$$\equiv AlOH \overset{K_2}{\leftrightarrow} \equiv AlO^- + H^+ \tag{2}$$

where, $\equiv AlOH$ represents the alumina surface. This is known as the 2 p*K* model (Yiacoumi and ChiTien, 1995) and K_1 and K_2 are the intrinsic equilibrium constants for Eqs. (1) and (2) respectively that describe the adsorption and desorption of protons. The charged surface concentrations are defined by Eqs. (3) and (4) as follows:

$$\left[\equiv AlOH_2^+\right] = K_1[\equiv AlOH]\{H^+\}\exp\left(\frac{-e\psi_o}{kT}\right) \tag{3}$$

$$\left[\equiv \mathrm{AlO}^-\right] = K_2[\equiv \mathrm{AlOH}]\left\{\mathrm{H}^+\right\}^{-1}\exp\left(\frac{e\psi_o}{kT}\right) \tag{4}$$

The terms within the parentheses [ ] define surface concentrations expressed in molarity units and terms within the parentheses { } define ionic solution concentrations in molarity units. The term $\exp(\frac{e\psi_o}{kT})$ takes into account the effect of the surface potentials at the adsorption plane. Here ψ_o is the surface potential, e is the electron charge, k is the Boltzmann constant, and T is the absolute temperature. The magnitude of the surface charge, i.e., degree of surface ionization, will depend on the acidic or basic strength of the functional groups or on pH of the solution. The positively charged surface will serve as surface site for fluoride complexation thereby removing fluoride from the aqueous medium. Therefore the binding of fluoride ions on to the alumina surface is described by the following complexation reaction:

$$\equiv \mathrm{AlOH}_2^+ + \mathrm{F}^- \overset{K_f}{\leftrightarrow} \equiv \mathrm{AlOH_2F}^0 \tag{5}$$

K_f is defined as the equilibrium constant for the adsorption reaction of Eq. (5) and the concentration of adsorbed fluoride is:

$$\left[\equiv \mathrm{AlOH_2F}^0\right] = K_f\left[\equiv \mathrm{AlOH}_2^+\right]\left\{\mathrm{F}^-\right\} \tag{6}$$

The extent of fluoride adsorption on the alumina surface (assuming it to be spherical) is defined by the term the fractional coverage τ, as:

$$\tau = \frac{\left[\equiv \mathrm{AlOH_2F}^0\right]}{[\equiv \mathrm{AlOH}] + \left[\equiv \mathrm{AlOH}_2^+\right] + \left[\equiv \mathrm{AlO}^-\right] + \left[\equiv \mathrm{AlOH_2F}^0\right]} \tag{7}$$

By incorporating Eqs. (3), (4) and (6) into Eq. (7), it becomes equivalent to:

$$\tau = \frac{K_f K_1\{\mathrm{H}^+\}\{\mathrm{F}^-\}\exp(\frac{-e\psi_o}{kT})}{1 + K_f K_1\{\mathrm{H}^+\}\{\mathrm{F}^-\}\exp(\frac{-e\psi_o}{kT}) + K_1\{\mathrm{H}^+\}\exp(\frac{-e\psi_o}{kT}) + K_2\{\mathrm{H}^+\}^{-1}\exp(\frac{e\psi_o}{kT})} \tag{8}$$

Aluminium from the alumina surface may get dissolved based on its equilibrium solubility in water and the equilibrium formation of its dissolved fluoride, hydroxyl fluoride and hydroxide forms. The total dissolved aluminium from the alumina surface is defined as $\mathrm{Al_D}$ and its concentration is determined by considering the formation of the dissolved free aluminium ions, various aluminium fluoride complexes (AlF^{2+}, AlF_2^+, AlF_4^-, AlF_5^{2-} and AlF_6^{3-}), aluminium hydroxides (AlOH^{2+}, $\mathrm{Al(OH)}_2^+$, $\mathrm{Al(OH)}_4^-$ and $\mathrm{Al_2(OH)}_2^{2+}$) and aluminium hydroxyl fluoride like AlOHF^+ and $\mathrm{Al(OH)_2F}_2^-$ complexes. The solubility of aluminium oxides in the aqueous medium is defined by the solubility product K_{SP} and the concentration of the various aluminium complexes estimated on the basis of their thermodynamic reaction equations are detailed in Table 1. Presence of high concentrations of complexing fluoride ligands and low pH, favor the formation of aluminium fluoride complexes AlF^{2+} and AlF_2^+ and increase the residual aluminium. The neutrally charged aqueous complexes that can be formed during the process include complexes like AlF_3^0, AlOHF_2^0, $\mathrm{Al(OH)_2F}^0$ and $\mathrm{Al(OH)}_3^0$, and their concentrations are considerable at pH values of 6–7 when fluoride concentrations are high and therefore increase residual aluminium concentrations.

The equation for the total dissolved aluminium is defined as:

$$\begin{aligned}\{\mathrm{Al_D}\} = {} & \left\{\mathrm{Al}^{3+}\right\} + \left\{\mathrm{AlF}^{2+}\right\} + \left\{\mathrm{AlF}_2^+\right\} + \left\{\mathrm{AlF}_4^-\right\} + \left\{\mathrm{AlF}_5^{2-}\right\} \\ & + \left\{\mathrm{AlF}_6^{3-}\right\} + \left\{\mathrm{AlOHF}^+\right\} + \left\{\mathrm{Al(OH)_2F}_2^-\right\} + \left\{\mathrm{AlOH}^{2+}\right\} \\ & + \left\{\mathrm{Al(OH)}_2^+\right\} + \left\{\mathrm{Al(OH)}_4^-\right\} + 2\left\{\mathrm{Al_2(OH)}_2^{2+}\right\}\end{aligned} \tag{9}$$

The total available surface for adsorption is calculated after considering the dissolution of alumina. Therefore the decrease in the mass of alumina due to aluminium dissolution is defined as:

$$m = m_0 - \left(\frac{\{\mathrm{Al_D}\} \times 27}{0.53}\right) \tag{10}$$

where, m_0 is the initial weight of adsorbent alumina in grams, and $\mathrm{Al_D}$ is dissolved aluminium from alumina surface in molar concentrations.

The surface charge density σ_o and surface potential ψ_o on the alumina surface are related by the Gouy–Chapman theory (Yiacoumi and ChiTien, 1995) of diffuse layer as:

$$\sigma_o = \sqrt{8\varepsilon RTI}\sin h\left(\frac{e\psi_o}{2kT}\right) \tag{11}$$

where I is the ionic strength and ε is the permittivity of the aqueous medium, and R is the gas constant. The surface charge density σ_o is defined in terms of the surface charge concentration as:

$$\sigma_o = N\left\{\left[\equiv \mathrm{AlOH}_2^+\right] - \left[\equiv \mathrm{AlO}^-\right]\right\} \tag{12}$$

where N is the conversion factor given by $N = F/Am$ and F is the Faraday constant, A is the surface area of alumina per unit weight and m is the mass of adsorbent alumina.

After incorporating Eqs. (3), (4) and (10) into Eq. (12) it is rewritten as:

$$\sigma_o = \frac{F[\equiv \mathrm{AlOH}]\left(K_1\{\mathrm{H}^+\}\exp(\frac{-e\psi_o}{kT}) - K_2\{\mathrm{H}^+\}^{-1}\exp(\frac{e\psi_o}{kT})\right)}{\left(m_0 - \left(\frac{\{\mathrm{Al_D}\}\times 27}{0.53}\right)\right)A} \tag{13}$$

The total site density N_S (in mols/m^2), including the different surface groups is given as:

$$N_S = \frac{N}{F}\left([\equiv \mathrm{AlOH}] + \left[\equiv \mathrm{AlOH}_2^+\right] + \left[\equiv \mathrm{AlO}^-\right] + \left[\equiv \mathrm{AlOH_2F}^0\right]\right) \tag{14}$$

Incorporating Eqs. (3), (4), (6) and (10) into Eq. (14), the concentration of the surface site $\equiv$AlOH is given by:

$$[\equiv \mathrm{AlOH}] = \frac{N_S\left(m_0 - \left(\frac{\{\mathrm{Al_D}\} \times 27}{0.53}\right)\right)A}{1 + K_f K_1\{\mathrm{H}^+\}\{\mathrm{F}^-\}\exp(\frac{-e\psi_o}{kT}) + K_1\{\mathrm{H}^+\}\exp(\frac{-e\psi_o}{kT}) + K_2\{\mathrm{H}^+\}^{-1}\exp(\frac{e\psi_o}{kT})} \tag{15}$$

Table 1 – Thermodynamic stability constants for formation of Al–OH, Al–F and Al–OH–F Complexes (pK values are for 25 °C and 0 Ionic strength).

Reaction equations	pK values	References	Concentrations of the aluminium complexes
$Al(OH)_3\ (s) = Al^{3+} + 3OH^-$	32.3	(Bi et al., 2001)	$\{Al^{3+}\} = \frac{K_{SP}}{(K_w/\{H^+\})^3}$
$Al^{3+} + H_2O = AlOH^{2+} + H^+$	4.99	(Nordin et al., 1999)	$\{AlOH^{2+}\} = 10^{-4.99}\{Al^{3+}\}/\{H^+\}$
$Al^{3+} + 2H_2O = Al(OH)_2^+ + 2H^+$	10.1	(Nordin et al., 1999)	$\{Al(OH)_2^+\} = 10^{-10.1}\{Al^{3+}\}/\{H^+\}^2$
$Al^{3+} + 3H_2O = Al(OH)_3\ (aq) + 3H^+$	16.9	(Nordin et al., 1999)	$\{Al(OH)_3^0\} = 10^{-16.8}\{Al^{3+}\}/\{H^+\}^3$
$Al^{3+} + 4H_2O = Al(OH)_4^- + 4H^+$	23.0	(Nordin et al., 1999)	$\{Al(OH)_4^-\} = 10^{-23}\{Al^{3+}\}/\{H^+\}^4$
$2Al^{3+} + 2H_2O = Al_2(OH)_2^{2+} + 2H^+$	−6.3	(Nordin et al., 1999)	$\{Al_2(OH)_2^{2+}\} = 10^{+6.3}\{Al^{3+}\}^2/\{H^+\}^2$
$Al^{3+} + F^- = AlF^{2+}$	−7.0	(Tagirov and Schott, 2001; Tagirov et al., 2002)	$\{AlF^{2+}\} = 10^{+7}\{Al^{3+}\}\{F^-\}$
$Al^{3+} + 2F^- = AlF_2^+$	−11.1	(Tagirov and Schott, 2001; Tagirov et al., 2002)	$\{AlF_2^+\} = 10^{11.1}\{Al^{3+}\Big\}\{F^-\}^2$
$Al^{3+} + 3F^- = AlF_3(aq)$	−16.8	(Tagirov and Schott, 2001; Tagirov et al., 2002)	$\{AlF_3^0\} = 10^{+16.8}\{Al^{3+}\Big\}\{F^-\}^3$
$Al^{3+} + 4F^- = AlF_4^-$	−19.4	(Tagirov and Schott, 2001; Tagirov et al., 2002)	$\{AlF_4^-\} = 10^{+19.4}\{Al^{3+}\Big\}\{F^-\}^4$
$Al^{3+} + 5F^- = AlF_5^{2-}$	−20.6	(Tagirov and Schott, 2001; Tagirov et al., 2002)	$\{AlF_5^{2-}\} = 10^{+20.6}\{Al^{3+}\Big\}\{F^-\}^5$
$Al^{3+} + 6F^- = AlF_6^{3-}$	−20.6	(Nordin et al., 1999)	$\{AlF_6^{3-}\} = 10^{+20.6}\{Al^{3+}\Big\}\{F^-\}^6$
$Al^{3+} + F^- + H_2O = AlOHF^+ + H^+$	0.0	(Nordin et al., 1999)	$\{AlOHF^+\} = \{Al^{3+}\}\{F^-\}/\{H^+\}$
$Al^{3+} + 2F^- + H_2O = AlOHF_2^0 + H^+$	−20.6	(Nordin et al., 1999)	$\{AlOHF_2^0\} = 10^{20.6}\frac{\{Al^{3+}\}\{F^-\}^2}{\{H^+\}}$
$Al(OH)_4^- + 2F^- = Al(OH)_2F_2^- + 2OH$	7.21	(Nordin et al., 1999)	$\{Al(OH)_2F_2^-\} = 10^{-7.2}\frac{\{AlOH^{4-}\}\{F^-\}^2}{\{OH^-\}^2}$

The overall fluoride mass balance is obtained by considering the dissolved free and complexed fluorides, the neutrally charged fluorides and the fluoride adsorbed on the alumina surface. The fluoride distribution is defined as:

$$\begin{aligned}\{F_{TOTAL}\} =& \{F^-\} + \left\{AlF^{2+}\right\} + 2\left\{AlF_2^+\right\} + 3\{AlF_3\} + 4\left\{AlF_4^-\right\} \\ &+ 5\left\{AlF_5^{2-}\right\} + 6\left\{AlF_6^{3-}\right\} + \left\{AlOHF^+\right\} + 2\left\{AlOHF_2^0\right\} \\ &+ \{Al(OH)_2F^0\} + 2\{Al(OH)_2F_2^-\} + [\equiv AlOH_2F^0] \qquad (16)\end{aligned}$$

Eqs. (8), (9), (11),(13), (15) and (16) constitute the system of equations describing the defluoridation mechanism on alumina in combination with dissolution of aluminium from the alumina surface. These six equations are simultaneously solved for determining the 6 unknowns $[\equiv AlOH], \psi_o, \{Al_D\}, \sigma_o, \{F^-\}$ and τ, when all the other parameters K_{SP}, K_f, K_1, K_2, N_S, m_0, A, I and $\{H^+\}$ are known. The AAD model uses the solubility product value (K_{SP}) of 10^{-32} which is applicable for the most stable form of aluminium hydroxides/oxides like gibbsite or alumina. Parameters K_f, K_1, K_2 and N_S are fitting parameters in the model, and their values are obtained from literature or experimental studies or chosen such that the experimental and simulated results for concentrations of residual aluminium and residual fluoride in defluoridation converged. The objective function for obtaining best fit for K_f is defined as given in Eq. (17).

$$\text{ObjF}_{K_f} = \left(\left(\sum_{i=1}^{NP}(F_{i\ sim} - F_{i\ exp})^2\right)\Big/ NP\right)^{0.5} \qquad (17)$$

Here NP is the number of data points, and $F_{i\ sim}$ and $F_{i\ exp}$ are the simulated and the experimental values of residual fluoride concentrations for a data point i. The approximate value for K_f, was also determined from experimental secondary data of Selvapathy and Arjunan (1995) and K_f was calculated using Eq. (18) which was obtained from the mass balances for aluminium and fluoride concentrations.

$$K_f = \frac{\{F_T\} - \{F^-\}}{\{F^-\}[(\{Al_T\} - \{Al_D\}) - (\{F_T\} - \{F^-\})]} \qquad (18)$$

Fig. 1 depicts the pK_f values estimated at different values of pH for different sample dosages of alum and fluoride and estimated to be around 4.0 for pH ranging from 5 to 8. The value of pK_f for surface complexation of monovalent inorganic anions for activated alumina was reported at 6.7–6.8 by Todorovic and Milonjovic (2004) and Tagirov et al. (2002) had also reported pK_f value of 5.5 for alumina for fluoride complexation. Objective function for fitting the intrinsic ionization equilibrium constants K_1 and K_2 is defined as given in Eq. (19).

$$\text{ObjF}_K = \left(\left(\sum_{i=1}^{NP}(Al_{i\ sim} - Al_{i\ exp})^2\right)\Big/ NP\right)^{0.5} \qquad (19)$$

where $Al_{i\ sim}$ and $Al_{i\ exp}$ are the simulated and the experimental values of residual aluminium concentrations for a data point i. Approximate values of K_1 and K_2 were also obtained using the definitions $pK_1 = (pH_{pzc} - \Delta pK/2)$, $pK_2 = (pH_{pzc} + \Delta pK/2)$ and $\Delta pK = (pK_2 - pK_1)$. The point of zero charge (pH_{pzc}) of alumina FB101 was experimentally obtained at a value of 8 as shown in Fig. 2. Todorovic and Milonjovic (2004) reported that for γ-alumina having point of zero charge at pH 7.2, the value of site density N_S is at 8 sites/nm^2 and the values of the intrinsic equilibrium constants i.e., pK_1 and pK_2 are at 4.4 and 9.6 respectively. The values of the equilibrium constants fitted into this simulator were $K_1 = 10^{-5}$, $K_2 = 10^{-11}$, $K_f = 10^{-5}$ and $N_S = 8$ sites/nm^2 for $\text{ObjF}_{KF} = 0.66$ (from 24 data points) and $\text{ObjF}_{AL} = 0.85$ (from 14 data points). A computer program was developed for the AAD model Simulator in the FORTRAN language using a Pentium IV

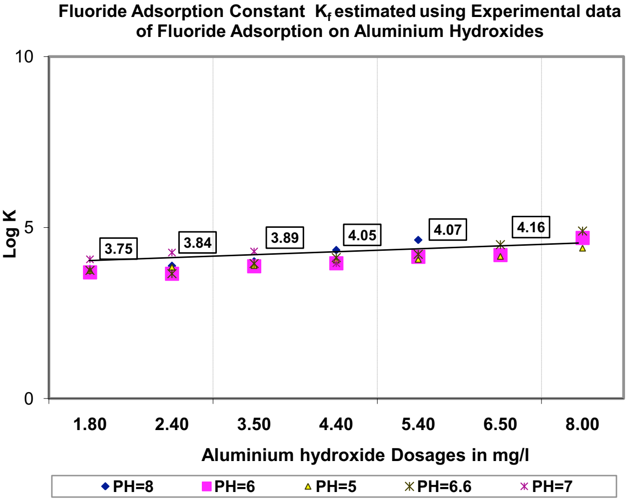

Fig. 1 – Fluoride adsorption constant K_f estimated using experimental data of fluoride adsorption on aluminium hydroxides.

personal computer configured with 128 MB memory and Fortran77 compiler. All calculations were done in double precision. The simulator program used Newton's method for solving the set of highly nonlinear model equations and iterations were performed until convergence to the desired level (i.e., the difference between last consecutive values is 10^{-6}) was reached for the material balances. Fig. 3 presents the flow diagram of the developed computer based AAD simulator. The AAD simulations estimate for the overall residual aluminium and residual fluoride concentrations, as well as for the concentrations of all ionic aluminium fluoride and aluminium hydroxyl fluoride complexes in the dissolved and precipitated forms in the alumina treated water with respect to varying raw water fluoride concentrations, alumina dosage and pH during defluoridation.

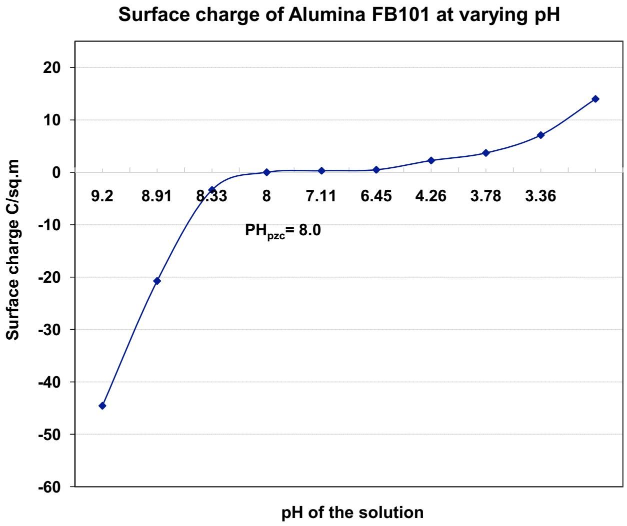

Fig. 2 – Surface charge of Alumina FB101 at varying pH.

3. Experimental materials and methods

3.1. *Batch studies of defluoridation with activated alumina grade FB101*

Batch defluoridation experiments were carried out using specific dosages of alumina treating varying fluoride water solutions for AAD Simulator validation. The activated alumina used for defluoridation was procured from Bharghava Industries Limited, Surat, of grade FB101. The specifications of the alumina are given in following Table 2. The adsorbent was washed with distilled water prior to conducting the experiments and synthetic sodium fluoride was used as the fluoride source. All chemicals, buffers used were of AR grade of Merck. Dilute solutions of 0.1 N NaOH and HNO_3 were used for pH adjustments. Filtration of solutions was carried out using a vacuum pump and a membrane filter assembly fitted with 0.45 μm cellulose acetate membrane filters and fresh membranes were used for every sample. The concentrations of residual fluoride and residual aluminium in the filtrate were determined. All samples were prepared and handled in polypropylene bottles, flasks, cylinders etc to prevent fluoride leaching.

Analysis of residual aluminium in defluoridated water was done using an Atomic Absorption Spectrophotometer (AAS) (Make-GBC Scientific Equipment, Australia, Model-Avanta) with acetylene-nitrous oxide flame furnace with D2 arc background corrector. The working range of the instrument for aluminium was 0.3–100 mg/L with wave length of 396.2 nm and lamp current of 10 mA. The range of absorbance was 0.1–0.5 for 2–10 mg/L Al and RSD was within 2% with good repeatability. Standard Al solutions of 1, 2, 4, 6, 8 and 10 mg/L concentrations were prepared using standard reference (stock) solution of 997 mg/L (Merck), and distilled water was used for preparation of standards and dilution of solutions. Potassium Chloride (2000 mg/L) was added to all the standards and samples to prevent the ionization of aluminium during Al determinations. Digestion procedure for solubilization of the precipitated forms of Al was done by lowering sample pH to 1 using trace metal grade nitric acid and keeping it for 2 h before measurement.

The residual fluoride in the alumina treated solutions was analyzed using an Ion Analyser (make-Mettler Toledo) and coupled to a standard electrode as reference. Calibrations were done using fluoride standards and the electrode slope was kept at −59.16±3 mv/decade at 25 °C. Standard fluoride solutions of 2, 4, 6, 8, 10 mg/L etc. were prepared from standard stock solution of 1000 mg/L using distilled water. For decomplexation of aluminium complexes and avoiding interference with the electrode performances, an ionic strength fixer and buffer TISAB-II solution set to a pH in the range 5.0–5.3 with 6 N NaOH, was added during measurements to the samples and standards. The TISAB solution was added in the proportion of 1:1 to 20 ml of sample and allowed to stand for 2 h at 25 °C before the electrode readings were taken. The standards and samples were also stirred at uniform rate (Magnetic Stirrer Remi make, Model MS500, speed 60 rpm) and the temperature was also maintained constant. The calibration was checked in between the

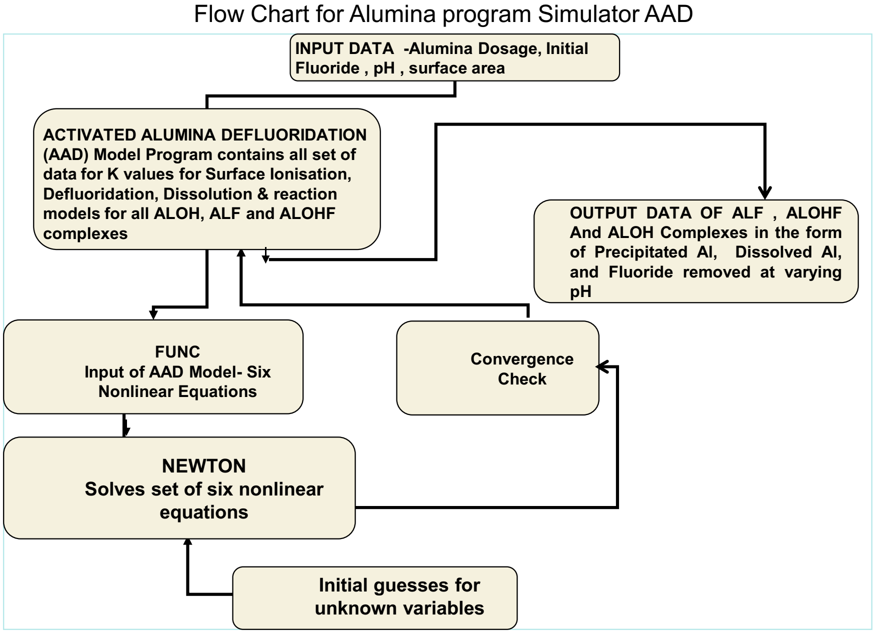

Fig. 3 – Flow chart for Alumina program Simulator AAD.

measurement of the fluoride samples. Potentiometric titrations were conducted in a Automatic Potentiometric Titrator (make-Spectralab, Model AT38C) to determine surface charge and point of zero charge of alumina. Two titrations were carried out: one in the presence of alumina (92 mg Al_2O_3) in 10 ml aqueous electrolyte solution of various concentrations and the other with the same electrolyte but in the absence of alumina (blank). Sodium chloride was used as supporting electrolyte and solutions of either HCl or NaOH (both 0.1 N) were used as the titrant for pH range from 6 to 10. Lower pH ranges were not done as they only solubilised the alumina. Care was taken to ensure constant temperature ($25 \pm 0.5\ ^{\circ}C$) during the experiment and enough time was given so that the solid and the bulk solution were in equilibrium allowing diffusive mixing. Deionised water-Lichrisolv (Merck) was used during the potentiometric titrations.

Table 2 – Specifications of FB101 grade alumina.

S No	Particulars	Specification
1.	Particle form	Spherical
2.	Particle size (mm)	0.4–1.2 mm
3.	Water adsorption capacity at 30°C and 60%RH by weight	19.83
4.	Surface area sq.m/gm (minimum)	260
5.	Pore volume cc/gm	0.43
6.	Bulk density gm/cc	0.82–0.87
7.	Bed crushing strength %	99.8
8.	Loss on attrition	0.145
9.	Loss on ignition (250°C to 1000°C)	7.33
10.	Chemical analysis	
	Al_2O_3 by difference	92.34
	Na_2O	0.10
	Fe_2O_3	0.03
	SiO_2	0.03

4. Results and discussion

4.1. *Effect of pH on residual fluoride and aluminium concentrations*

The simulated and experimental results for residual aluminium and fluoride concentrations in the defluoridated water, obtained on treating 200–1000 mg of alumina in 100 ml fluoride water of different fluoride concentrations 4, 6, 8, 10 mg/L and at varying pH conditions of 5, and 7 are presented in Table 3. The residual aluminium concentrations for varying pH are also presented in Fig. 4. The total residual aluminium in the defluoridated water is due to sum of both dissolved and precipitated complexed forms, as the precipitated AlF are monomeric forms and not removed during filtration by a 0.45 μm membrane. Similarly the residual fluoride is due to fluoride present in free and complexed forms (both dissolved and precipitated Al–F complexes). At conditions of pH 7, the simulation results gave low dissolved aluminium concentrations varying from 0.2 to 0.4 mg/L. However the formation of the neutrally charged AlF_3^0, $AlOHF_2^0$ and $Al(OH)_2F^0$ precipitates were predominant at this pH, and increased significantly with increase in fluoride concentrations. For a 10 mg/L fluoride solution these precipitated forms induced 2.18 mg/L of residual fluoride and 1.04 mg/L of residual aluminium into the treated water. Hence the total residual aluminium was higher at 1.42 mg/L. The total residual fluoride, as per model predictions, would predominantly be due to the presence of free fluoride ions and the complexed form of AlF_2^+ which is preferentially formed at this pH. The fluoride removal efficiencies

Table 3 – Residual fluoride and aluminium concentrations on batch defluoridation treating different dosages of Activated Alumina (AA) in 100 ml fluoride solution at varying pH.

Initial F Conc. mg/L	AA in mg	pH	Simulated			Exp.	Simulated				Exp.	% F removed
			Fdis	Fppt	Total Fres	Fexp	Fads	Aldis	Alppt	Total Alres	Alexp	
4	200	7	3.29	0.27	3.56	3.3	0.44	0.11	0.13	0.24	0.9	11.0
6	200	7	4.67	0.72	5.39	4.6	0.61	0.19	0.37	0.56	1.1	10.2
8	200	7	5.87	1.37	7.24	6.7	0.76	0.28	0.66	0.94	1.5	9.50
10	200	7	6.91	2.18	9.13	8.2	0.88	0.38	1.04	1.42	1.7	8.80
4	200	5	3.97	0.029	3.99	3.4	0.004	4.7	0.016	4.722	4.4	0.10
6	200	5	5.934	0.0608	5.994	5.9	0.005	6.4	0.03	6.43	6.8	0.09
8	200	5	7.893	0.10	7.99	6.5	0.006	8.05	0.05	8.10	8.0	0.07
10	400	7	6.512	1.837	8.34	7.2	1.651	0.33	0.97	1.20	1.50	16.52
10	500	7	6.31	1.682	7.99	7.1	2.01	0.315	0.80	1.115	1.1	20.10
10	800	7	5.75	1.29	7.04	6.5	2.96	0.27	0.62	0.89	1.0	30.0
10	1000	7	5.41	1.09	6.50	–	3.50	0.24	0.52	0.76	–	34.9

$\mathrm{Fdis} = [\{F^-\} + \{AlF^{2+}\} + 2\{AlF_2^+\} + 4\{AlF_4^-\} + 5\{AlF_5^{2-}\} + 6\{AlF_6^{3-}\} + \{AlOHF^+\} + 2\{Al(OH)_2F_2^-\}]$
$\mathrm{Fppt} = [3\{AlF_3^0\} + 2\{AlOHF_2^0\} + \{Al(OH)_2F^0\}]$
Total Fres = Fdis + Fppt, Fads = fluoride adsorbed on alumina as $[\equiv AlOH_2F^0]$

$\mathrm{Aldis} = [\{Al^{3+}\} + \{AlF^{2+}\} + \{AlF_2^+\} + \{AlF_4^-\} + \{AlF_5^{2-}\} + \{AlF_6^{3-}\} + \{AlOHF^+\} + \{Al(OH)_2F_2^-\} + \{AlOH^{2+}\} + \{Al(OH)_2^+\} + \{Al(OH)_4^-\} + 2\{Al_2(OH)_2^{2+}\}]$
$\mathrm{Alppt} = [\{AlF_3^0\} + \{AlOHF_2^0\} + \{Al(OH)_2F^0\} + \{Al(OH)_3^0\}]$
Total Alres = Aldis + Alppt

were very low at only 9–10% for low dosages of 200 mg/L of alumina. The comparison for simulated and experimental data given in Table 3, indicates that the predicted values for the model were within ±5% of the experimental results, validating the AAD model simulator.

The alumina surfaces being amphoteric in nature, ionize to form both positively and negatively charged surfaces according to the pH of the solution. The point of zero charge of the alumina was experimentally found to be at 8, hence the alumina surfaces were forming positively charged sites in the region of 7–8 and adsorbing the negatively charged fluoride ions causing better fluoride removal. Lowering the pH to 5 favored the formation of dissolved Al–F and Al–F–OH complexes and hence increased the residual aluminium and fluoride concentrations. The residual aluminium concentrations were approx 4.4, 6.8, and 8.1 mg/L at pH of 5 for fluoride solutions of 4, 6 and 8 mg/L respectively. Each aluminium ion being complexed with one or more fluoride ions, residual fluoride concentrations were also proportionately higher with respect to residual aluminium concentrations. Hence fluoride removal by adsorption on to the alumina surfaces was negligible as 90% of the fluoride remained in the solution in its complexed forms with aluminium. In alkaline pH, fluoride remains as free F-ions, as the aluminium ions will

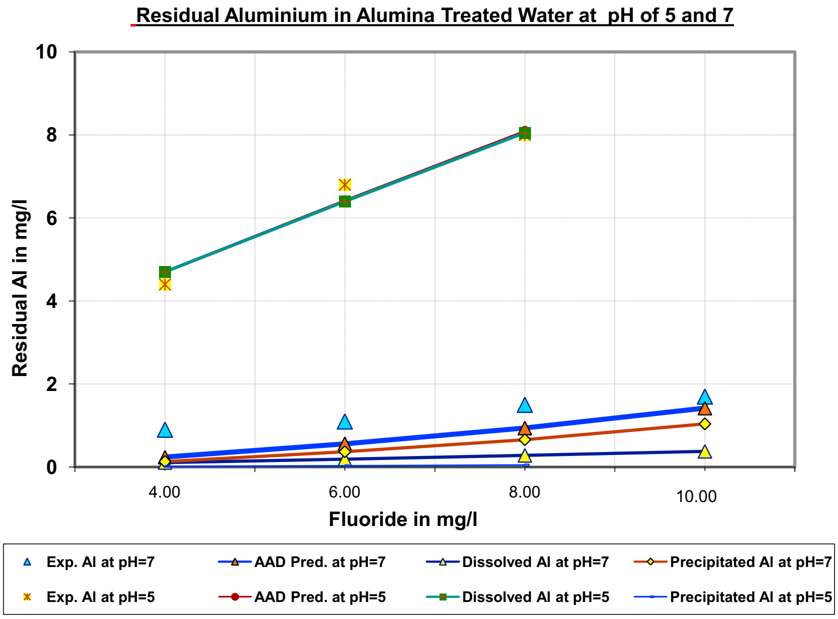

Fig. 4 – Residual aluminium in alumina treated water at pH of 5 and 7.

preferentially form their hydroxide forms. Fluoride adsorption will decrease as the alumina surface sites are negatively charged in the alkaline medium and repel the negatively charged fluoride ions. The dissolved aluminium again increases due to the formation of its dissolved tri-hydroxides in alkaline conditions.

4.2. *Effect of increase in alumina dosages*

As the % fluoride removal for 200 mg dosage of alumina was very small, hence experiments were conducted with 100 ml of 10 mg/L fluoride solutions treated with increasing doses such as 200, 400, 500, 800 and 1000 mg of alumina at pH 7. The fluoride removal increased from 18 to 35% as the dosage increased from 200 to 1000 mg of alumina and the % distribution of fluoride, for adsorbed, precipitated and dissolved forms is shown in Fig. 5. The residual aluminium concentrations decreased with increased alumina dosages because formation of neutral precipitates AlF_3^0, $AlOHF_2^0$ and $Al(OH)_2F^0$ decreased as more of fluoride was preferentially adsorbed on to alumina surfaces. When higher alumina dosages are used to treat the same quantity of fluoride, it does not proportionately increase the aluminium concentration in water. This is because during the defluoridation process there are two mechanisms that occur simultaneously, i.e., the aluminium dissolution due to interactions of fluoride ions with aluminium ions and the fluoride adsorption mechanism. The residual aluminium concentrations in treated water are defined by the thermodynamic equilibrium of the alumina solubility reaction and the aluminium fluoride reactions. High concentrations of fluoride will increase the formation of aluminium fluoride complexes and hence the solubility of aluminium. However the availability of more surface sites on alumina will cause fluoride adsorption to occur preferentially over the dissolution mechanism. This is because the adsorption equilibrium is more favored than Al–F interaction as per thermodynamic reactions shown in Table 1.

4.3. *Adsorption isotherms*

The best pH range for fluoride adsorption on alumina is around pH 7–7.5, with high fluoride removal efficiency and minimum residual aluminium. Experiments were conducted with 4 different 100 ml fluoride solutions of 9.3, 7.9, 4.8 and 3.1 mg/L and treated with constant dosage 500 mg of alumina at pH 7.5. As the concentration of fluoride increases, more of monomeric AlF_3^0 is formed. Fig. 6 presents the comparison of experimental and simulated residual fluoride concentrations. There is an increase in residual aluminium concentrations and corresponding decrease in fluoride removal efficiency with increase in fluoride concentrations. These data was fit into the Freundlich adsorption isotherm which is indicative of the surface heterogeneity of the adsorbent and is shown in Fig. 7. The relationship is given by the linearised equation $\log(x/m) = \log k + (1/n)\ \log C_e$ where k and $1/n$ are the Freundlich constants related to the adsorption capacity and intensity respectively. Here C_e is the residual fluoride concentrations (mg/L) and x/m is the mg of fluoride adsorbed per gram of alumina. The value of k is 0.15 mg/g and $1/n$ is 0.45 and value of $1/n$ less than unity indicates favorable adsorption. The relationship is linear in the region of low fluoride concentrations, but as concentrations of fluoride increased, the formation of

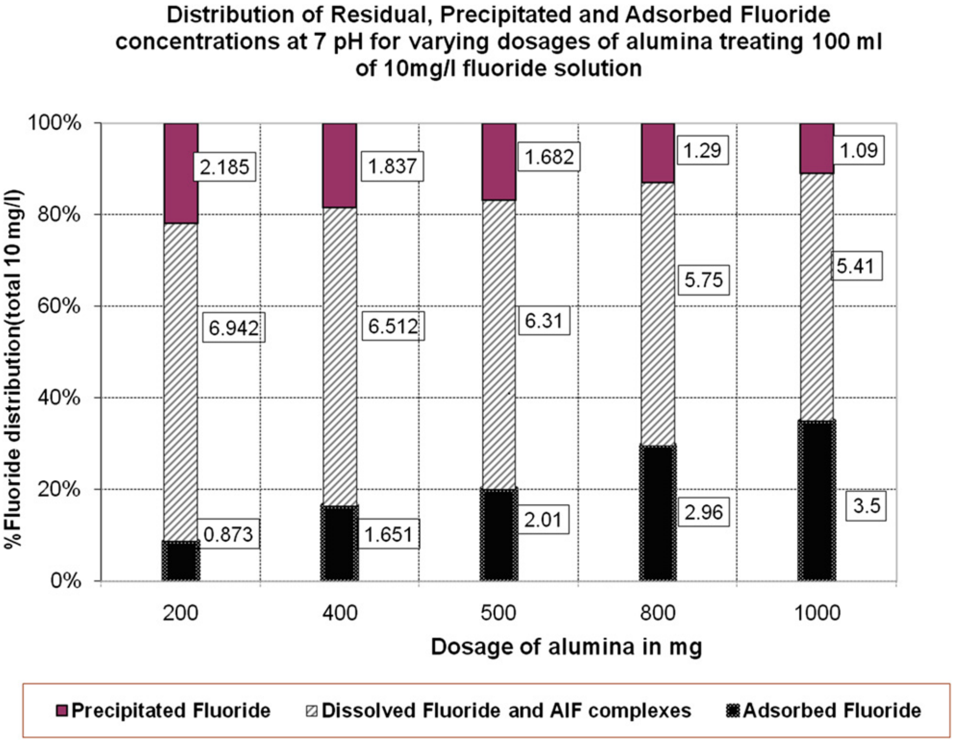

Fig. 5 – Distribution of Residual, Precipitated and Adsorbed fluoride concentrations at 7 pH for varying dosages of aluminatreating 100 ml of 10 mg/L fluoride solution.

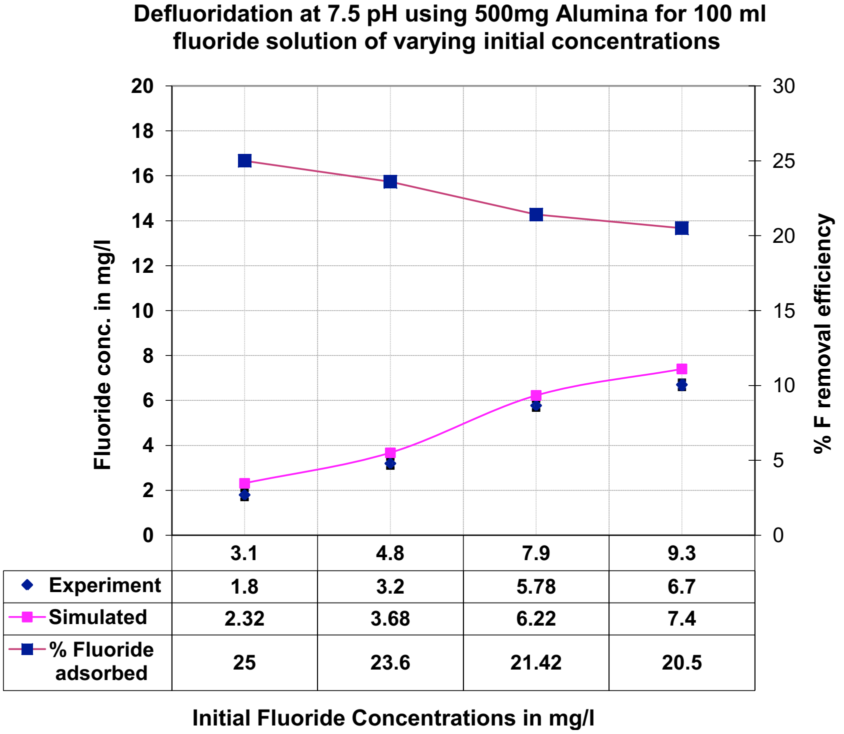

	3.1	4.8	7.9	9.3
◆ Experiment	1.8	3.2	5.78	6.7
■ Simulated	2.32	3.68	6.22	7.4
■ % Fluoride adsorbed	25	23.6	21.42	20.5

Fig. 6 – Defluoridation at 7.5 pH using 500 mg Alumina for 100 ml fluoride solution of varying initial concentrations.

the dissolved AlF_3^0 complexes was favored over adsorption on alumina, and hence makes it nonlinear for this pH.

The availability of sufficient surface sites for adsorption will keep the formation of the dissolved aluminium fluoride and aluminium hydroxyl fluoride complexes at its minimum as the adsorbent dosage is increased. Hence with higher alumina dosage, fluoride adsorption will preferentially occur and with low dosages of alumina treating high fluoride concentrations, aluminium dissolution will preferentially occur over adsorption. The developed AAD simulator can predict for residual fluoride, residual aluminium concentrations, extent of fluoride removal, etc for alumina dosages treating varying fluoride solutions at varying pH. Hence it is applicable for predicting minimum dosage of alumina or

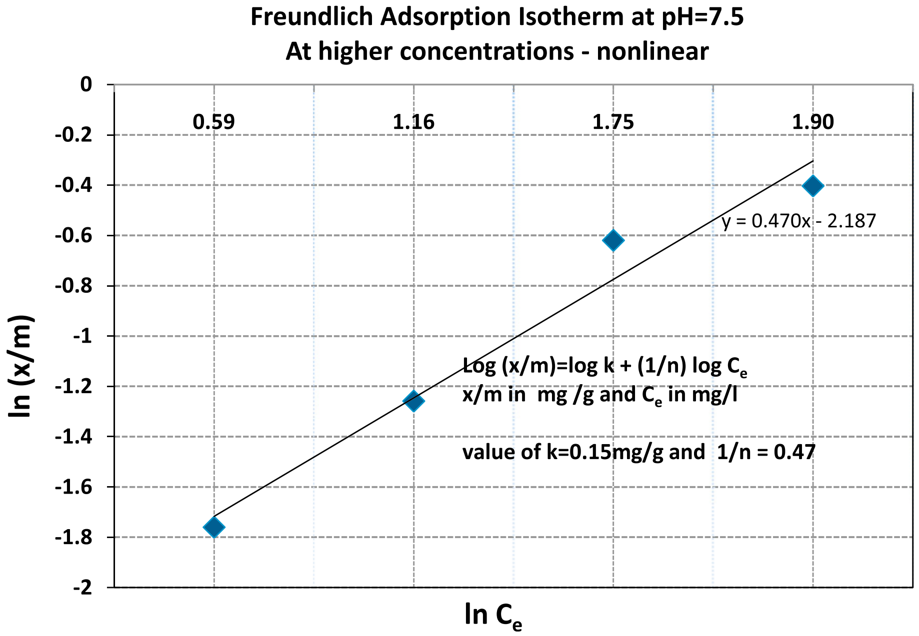

Fig. 7 – Freundlich adsorption isotherm at pH = 7.5 at higher concentrations – nonlinear.

fluoride uptake capacity that can produce minimum residual aluminium with better fluoride removal efficiencies.

5. Conclusion

Defluoridation on activated alumina was represented by AAD model simulator incorporating mechanism of dissolution of alumina surface with respect to pH changes and validated using residual aluminium and fluoride concentrations obtained from experimental studies. Activated alumina defluoridation process is found favorable for removal of fluoride, but identification of the optimum uptake capacity is essential so that fluoride adsorption is not offset by the aluminium dissolution mechanism on the alumina surface in presence of high fluorides. When fluoride concentrations are high and if low alumina dosages are used, the formation of AlF_3^0 is favored in pH range of 6.5–7.5, which may lead to increase in residual aluminium in treated water. Hence alumina dosages must be optimised at low fluoride uptake capacities, such that preferential adsorption of fluoride on alumina takes place. At higher uptake capacities, the formation of aluminium fluoride and aluminium hydroxyl fluoride complexes will increase the residual aluminium complexes. This also indicates that exhausted alumina surfaces may promote the dissolution of aluminium to form its dissolved fluoride complexes in the treated water. Hence regeneration cycles need to be fixed not only on the basis of bed exhaustion for fluoride uptake but also with respect to residual aluminium concentrations in treated water.

REFERENCES

Agarwal, K.C., Gupta, S.K., Gupta, A.B., 1999. Development of new low cost defluoridation technology (KRASS). Water Sci. Technol. 40 (2), 167–173.

Berend, K., Trouwborst, T., 1999. Cement mortar pipes as a source of aluminium. J. Am. Water Works Assoc. 91 (7), 91–100.

Bi, S.P., An, S.Q., Tang, W., Yang, M., Qian, H.F., Wan, J., 2001. Modeling the distribution of aluminium speciation in acid soil solution equilibria with the mineral phase alunite. Environ. Geol., 1–19 (Springer-Verlag).

Gauthier, E., Fortier, E., Courchesne, F., Pepin, P., Mortimer, J., Gauvreau, D., 2000. Aluminium Forms in Drinking Water and Risk of Alzheimer's disease. Environ. Res. 84, 234–246. Section A.

Feltes, T., Timmons, M., 2005. A Simple Procedure to Determine Surface Charging Parameters in Aqueous Solutions. Department of Environmental Sciences, University of California, Riverside, CA 92521, USA. Available from: www.uic.edu/labs/amrel/NSFREV02/final%20report/T.Feltes.&;M.Timmons.pdf.

Hiemstra, T., VanRiemsdijk, W.H., 2000. Fluoride Adsorption on Goethite in Relation to different types of surface sites. J. Colloid Interface Sci. 225, 99–104.

IS10500, 1991. Indian Standard Drinking Water Specification.

Kumar, J., Verma, V.K., 2004. Domestic defluoridation based on activated alumina technology – approach towards the development of generic code of practice. In: Proceedings of Workshop on Standardisation of Activated Alumina based Defluoridation Systems, 31st Aug to 1st Sept 2004, Organised by Rajasthan State PHED, GoR and UNICEF, Rajasthan.

Lefevre, G., Duc, M., Fedoroff, M., 2004. Effect of solubility on the determination of the protonable surface site density of oxyhydroxides. J. Colloid Interface Sci. 269, 274–282.

Martyn, C.N., Barker, D.J.P., Osmond, C., Harris, E.C., Edwardson, J.A., Lacey, R.F., 1989. Geological relation between Alzheimer's disease and aluminium in drinking water. The Lancet 1, 59–62.

McLachlan, D.R., Kruck, T.P., Lukiu, W.J., Krishnan, S.S., 1991. Would decreased aluminium ingestion reduce the incidence of Alzheimer's disease? Can. Med. Assoc. J. 145 (7), 796–804.

Nordin, J.P., Sullivan, David J., Phillips, Brian L., Casey, William H., 1999. Mechanisms for fluoride-promoted dissolution of bayerite [b-Al(OH)3 (s)] and boehmite [g-AlOOH]: 19 F-NMR spectroscopy and aqueous surface chemistry. Geochim. Cosmochim. Acta 63 (21), 3513–3524.

Sanjuan, B., Michard, Gil, 1987. Aluminium hydroxide solubility in aqueous solutions containing fluoride ions at 50 °C. Geochim. Cosmochim. Acta 51 (7), 1823–1831.

Selvapathy, P., Arjunan, N.K., 1995. Aluminium residues in water. In: Third International Conference on Approximate Waste Management Technologies for Developing Countries, Feb. 25–26, Nagpur. Technical papers, vol. II.

Singh, B.P., Bhattacharjee, S., Besra, L., Sengupta, D.K., 2005. Electrokinetic and adsorption studies of alumina suspensions using Darvan C as dispersant. J. Colloid Interface Sci. 289, 592–596.

Strunecka, A., Patocka, 1999. Pharmacological and Toxicological effects of aluminofluoride complexes. Fluoride 32 (4), 2–242.

Tagirov, B., Schott, J., 2001. Aluminium speciation in crustal fluids revisited. Geochim. Cosmochim. Acta 65 (21), 3965–3992.

Tagirov, B., Schott, J., Harrichoury, J.C., 2002. Experimental study of aluminium–fluoride complexation in near-neutral and alkaline solutions to 300 °C. Chem. Geol. 184 (3–4), 30–31.

Todorovic, A.N., Milonjovic, S.K., 2004. Determination of intrinsic equilibrium constants at an alumina/electrolyte interface. J. Serb. Chem. Soc. 69 (12), 1063–1072.

USPHS, 1987. Drinking Water Standards. Public Health Services Publication, Washington, DC, p. 333.

Valdivieso, L., Reyes Bahena, J.L., Song, S., Herrera Urbina, R., 2005. Temperature effect on the zeta potential and fluoride adsorption at the α-Al2O3/aqueous solution interface. J. Colloid Interface Sci. Available from: www.elsevier.com/locate/jcis.

WHO, 1997. Environmental Health Criteria for Aluminium, vol. 194. World Health Organization, Geneva.

Yiacoumi, S., ChiTien, 1995. Kinetics of Metal Ion Adsorption from Aqueous solutions. Kluwer Academic Publishers, London.